

Context-aware Simopt-Power: Using structural data with simulation metadata to optimise FPGA designs

Eashan Wadhwa, Georgios Floros & Shanker Shreejith
Department of Electronic and Electrical Engineering, Trinity College Dublin
Dublin, Ireland
{wadhwa, florosg, shreejith.shanker}@tcd.ie

Abstract—Pre-implementation behavioural simulation routinely validates functional correctness, yet it also produces rich switching-activity traces that are typically discarded by FPGA computer-aided design (CAD) flows. Prior simulation-guided and power-aware FPGA optimisations demonstrate the promise of exploiting this metadata, but many rely on fixed thresholds, narrow decision heuristics, or limited design awareness, often incurring substantial area overhead. This paper presents Context-aware Simopt-Power, a simulator-guided optimisation framework that combines activity metadata with lightweight structural features (sequential proximity, logic-depth proxies, and fan-out estimates) to more precisely target high-impact regions of the netlist. We additionally remove empirically tuned constants, replacing them with architecture-aware parameters such as LUT size and mapping constraints, and evaluate trade-offs using power, delay, and a more useful metrics, area-delay product (AD) and power-delay product (PD). Implemented in an open-source Yosys/ABC flow and evaluated on the complex Koios deep-learning accelerator benchmarks, Context-aware Simopt-Power achieves an average 6.8% dynamic-power reduction while limiting LUT overhead to 11.2%, thus enabling a holistic design optimisation.

I. INTRODUCTION

FPGAs have achieved widespread adoption across different domains from data centres to edge devices, and embedded systems, primarily as they enable power efficient design implementations compared to off-the-shelf platforms. Among the contributors to FPGA power consumption, dynamic power, dominated by signal switching activity across the highly configurable logic and interconnect fabric, remains the most significant and difficult to control. Frequent toggling of wide datapaths and global routing resources amplifies capacitive charging losses, making switching activity a critical lever for reducing overall energy consumption without altering device voltage or frequency. Traditional FPGA CAD flows primarily focus on functional correctness and timing closure, often overlooking the rich switching activity data available from pre-implementation simulation. While behavioural simulation is routinely employed to verify functional correctness, it also yields detailed toggle-rate and timing metadata that conventional FPGA CAD flows leave unused. This metadata, if harnessed effectively, can inform targeted optimisations to reduce dynamic power consumption as proven in prior works [1]. However, integrating simulation-derived insights into synthesis and mapping remains challenging because modern FPGA fabrics are heterogeneous and routing-dominated, while the CAD flows are not natively optimised around behavioural activity

metadata. Prior work has explored switching-activity reduction through switching-graph constraints [2], clock-gating approaches [3][4], and other power-oriented gating heuristics [5]. These methods show the value of power-aware optimisation, but they do not tightly couple simulation metadata with structural cues for switching-aware FPGA restructuring. This has proven to be very beneficial - [6] leverages structural design representations to guide design-space exploration in high-level synthesis for latency designs. Similarly, [7] integrates synthesis-aware modelling while jointly considering multiple performance indicators during neural-network accelerator prototyping. Collectively, these works highlight the benefits of embedding structural awareness into optimisation workflows to achieve more balanced and effective design trade-offs. In [1], the authors exploit a simulation-driven switching-reduction technique and reported measurable power savings on sequential benchmarks. However, its implementation depends on fixed thresholds and ad hoc heuristics, leading to coarse optimisation and substantial area overhead. The absence of explicit structural awareness in the decision process also limits how effectively it can balance power reduction against downstream resource cost. In this work, we present **Context-aware Simopt-Power**, an enhanced framework that couples simulation-derived activity metadata with structural design information to enable more principled switching-activity optimisation. Our main contributions are as follows:

- **Context-aware Shannon splitting heuristic:** We extend the existing truth-table-based decomposition strategy with lightweight structural features, such as sequential proximity, logic depth proxies, and fan-out estimates to guide optimisation decisions. This enables targeted transformations within deep inter-register logic, guard-dominated regions, and wide, high-activity cones where switching suppression yields the greatest benefit.
- **Elimination of heuristic constants:** We remove empirically tuned thresholds and replace them with architecture-aware parameters (such as LUT sizing and mapping constraints), improving portability across FPGA families through systematic optimisation.
- **Area-Delay and Power-Delay metrics:** We adopt a more comprehensive evaluation metric that captures the joint impact of power, area and performance, providing a holistic metric for analysing trade-offs in overall design

efficiency.

II. IMPLEMENTATION

We build on the Shannon-decomposition-based truth-table splitting routine, described in [1], as the fundamental transformation, but refine its decision policy using structural features and eliminate fixed, hand-tuned thresholds. Simopt framework [8] first collects per-net toggle statistics during behavioural simulation, which serve as switching-activity estimates to highlight high-activity cones. Based on these estimates, we extract candidate cuts and apply activity guided transformations within specific logic cones from ABC’s (Yosys) internal AIG representation and cut-enumeration data structures, prior to final LUT binding. Specifically, the optimisations we introduce comprise: (i) context-aware Shannon cofactoring of high-toggle variables within selected cuts; (ii) selective logic duplication to localise switching and reduce glitch propagation; (iii) restructuring of wide, guard-dominated cones to reduce unnecessary reconvergence; and (iv) activity-weighted cut re-evaluation to favour implementations that lower estimated dynamic power while respecting LUT size constraints. The modified network is then returned to ABC’s standard mapping flow to produce the final netlist. Each of these optimisation components are described in the following subsections. Alg. 1 provides the pseudocode for the ABC-integrated context-aware Shannon splitting routine which we call TTCONTEXTUALDECOMPOSE. This algorithm evaluates a candidate cut and optionally applies Shannon-style cofactoring when the context-aware cost justifies the LUT overhead. .

A. Structural eligibility filter for deep sequential cones

We first constrain TTCONTEXTUALDECOMPOSE to prioritise cuts whose right-cut function (T) resides within deep, serialised combinational regions. In the ABC internal representation, a logic cone is classified as “large logic between flops” when it is part of a sequential path and its estimated cut depth (d) exceeds a LUT-aware minimum threshold. The depth metric is exposed through an augmented mapping-context variable within ABC. This restriction is motivated by dynamic-power considerations: deep combinational regions are evaluated every clock cycle and typically exhibit numerous internal nodes and reconvergent paths. Thus reducing switching at the cone output is more likely to propagate meaningful activity suppression throughout the surrounding datapath. Moreover, these regions better amortise the area overhead introduced by Shannon cofactoring. To ensure architectural portability, we avoid hard-coded constants and instead define ($K := \max(\text{lutSize}, 6)$) and ($d_{\min} := K + 2$). K denotes the effective LUT input size of the target FPGA architecture, derived from the mapper’s `lutSize` parameter with six set as the lower bound to ensure architectural portability. A +2 guard-band threshold was chosen, to ensure the sequential cones are sufficiently deep so that the expected switching reduction can amortise the split overhead when compared to other threshold values shown in Fig. 1. The split search is therefore enabled only when the condition (is sequential and the condition ($d \geq d_{\min}$))

holds, otherwise, TTCONTEXTUALDECOMPOSE terminates early without modifying (T).

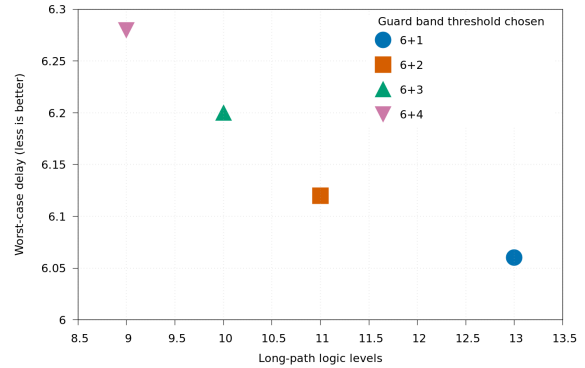


Fig. 1. A sweep scatter of various guard-band thresholds of worst-case delays vs logic levels on a critical path. +2 is the sweet spot for this architecture chosen with $K = 6$

B. Expected-activity model for sequential guard evaluation

In [1], the authors computed Shannon cofactors by enumerating the 2^n minterms of a truth table, where n is the truth-table size of the cut function. While exact, this brute-force view treats all cuts uniformly and does not exploit any per-cut context (e.g., whether the cone is sequential, or whether a split variable is likely to behave as a guard). To mitigate this, we introduce an *expected-ones-count model* in TTCONTEXTUALDECOMPOSE that estimates the activity of a Shannon split using a probabilistic prior, rather than assuming the quieter cofactor is always selected.

Let T denote the packed truth table of a cut on n variables, and let $N_1(T)$ be the number of minterms set to 1 in T (popcount of the truth-table bits). For a candidate split variable at position pos , we form the Shannon cofactors T_0 and T_1 by fixing the variable to 0 and 1, respectively. Define $N_0 := N_1(T_0)$ and $N_1 := N_1(T_1)$, and let $N_{\min} := \min(N_0, N_1)$ and $N_{\max} := \max(N_0, N_1)$. In prior optimisations, the split was implicitly modelled as if the quieter (i.e. the lower simopt-counter count) branch is always selected (i.e., the post-split ones-count equals N_{\min}). We instead model post-split activity by an expected value:

$$\mathbb{E}[N_{\text{after}}] := \pi N_{\min} + (1 - \pi) N_{\max}, \quad (1)$$

where $\pi \in [0.5, 0.95]$ is a prior probability that the *quiet* branch (the cofactor achieving N_{\min}) is taken at runtime. For purely combinational cones we set $\pi = 0.5$ (no bias), while for sequential cones we derive π from the Simopt score $s \in [0, s_{\max}]$, where s_{\max} is the second highest Simopt score observed after the clock nets.

$$\pi(s) := \text{clip}\left(0.95 - 0.45 \cdot \frac{s}{s_{\max}}, [0.5, 0.95]\right), \quad (2)$$

so that higher scores revert toward an unbiased (random) prior and lower scores permit a stronger guard-like bias toward the quiet branch. Finally, we define the expected improvement in ones-count as

$$\Delta N := N_1(T) - \mathbb{E}[N_{\text{after}}], \quad (3)$$

which is used as a switching-reduction proxy when ranking split candidates. This prevents the splitting of logic nets that are already low-activity, the split is only selected when the expected reduction in output activity (ΔN) is positive and large enough to amortise the estimated mux/duplication overhead. This component is primarily intended to model guard-dominated behaviour in deep sequential or glitch-prone cones.

C. LUT-aware overhead modelling

While Shannon decomposition can reduce switching activity, it also introduces structural overhead in the form of two cofactors and a selection function (conceptually, a mux). To avoid favouring splits that are unlikely to map efficiently, we incorporate a LUT-capacity term that reflects packing pressure. Let $n_{\text{new}} := |\mathcal{C}_{\text{new}}|$ denote the support size of the candidate cut and let K be the target LUT input capacity. When n_{new} approaches K , any additional logic created by the split is harder to absorb within a single LUT and is more likely to increase LUT count; conversely, when $n_{\text{new}} \ll K$, the mapping has slack and the overhead is typically easier to pack. We therefore apply a LUT-pressure factor P_{lut} that increases the overhead penalty as n_{new} nears (or exceeds) K , biasing the search towards decompositions that either (i) split near-capacity functions into smaller-support cofactors that map more cleanly, or (ii) avoid splits whose overhead would likely spill into additional LUTs. The illustration of the impact of these two parameters is shown in Fig. 2, where large area savings are possible for large cone depths.

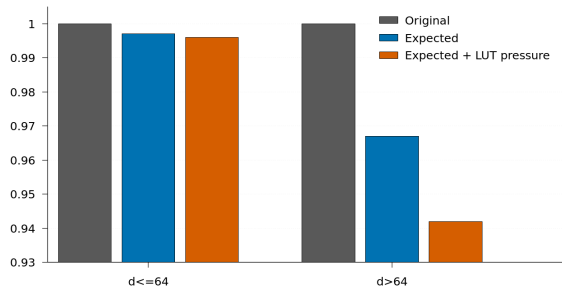


Fig. 2. Impact to area with Expected-value model optimisation (shown by the middle bar) and the Expected-value model with P_{lut} optimisations (the right-most bar) for *lstm.v*. The x-axis has two regimes: shallow cones ($d \leq 64$) and deep cones ($d > 64$), where d corresponds to the estimated sequential cone depth. Y-axis represents the normalised area impact.

D. Cofactor divergence penalty

If the two cofactors T_0 and T_1 are very large, then the decomposed output depends strongly on the split variable: toggling the split variable can cause many output minterms to change, which is undesirable when the goal is to reduce activity. We capture this effect by computing the XOR of the cofactors and counting how many minterms differ between them. Subsequently, we define a sensitivity penalty

$$P_{\text{sens}} := \cdot N_1(T_0 \oplus T_1),$$

Algorithm 1: TTCONTEXTUALDECOMPOSE

```

1 if not (isSequential ∧ d ≥ d_min) then
2   return T; // Structural eligibility not satisfied
3 foreach candidate variable x ∈ C do
4   compute ΔN; // Expected switching reduction from
   guard model
5   compute P_ovh; // Estimated overhead from LUT-aware
   model
6   compute P_sens; // Penalty from cofactor divergence
7   score ← ΔN − P_ovh − P_sens;
8   if score > bestScore then
9     bestScore ← score;
10    bestVar ← x;
11 if bestScore > 0 then
12   return TTDECOMPOSE(C, bestVar); // Without splitting
   logic from [1]
13 else
14   return T;

```

where $N_1(\cdot)$ is the number of ones (i.e., differing minterms) in the XOR truth table. This term discourages split variables that behave like a highly sensitive selector rather than a guard.

E. Final split score and decision rule

The components described above are combined into a single scalar score that balances expected switching reduction against structural penalties. Before evaluating any split candidates, we first apply the structural eligibility filter described in Section II-A. The contextual decomposition is attempted only if the cut lies in a sufficiently deep sequential cone, i.e. ($d \geq d_{\text{min}}$) where $d_{\text{min}} = K + 2$ and K is the effective LUT size. If this condition does not hold, the truth table T is left unchanged and no further evaluation is performed. For a candidate split variable, we compute the expected reduction in ones-count ΔN (Eq. 3) from Section II-B, the LUT-pressure penalty P_{lut} (from Section II-C), and the mux-sensitivity penalty P_{sens} (from Section II-D). The overall score is defined as

$$\text{score}(\text{splitVar}) := \Delta N - P_{\text{lut}} - P_{\text{sens}}. \quad (4)$$

We summarise this algorithm change in Algorithm 1. This new function is stitched into the existing Simopt Yosys-ABC flow at the cut-processing stage of technology mapping, where each candidate cut is evaluated. Once all cuts have been processed, ABC emits the mapped BLIF netlist, which can be imported into subsequent place and route stages. For our evaluation, we use Vivado to target FPGA implementations. We discuss this further in Sec. III

III. RESULTS

To evaluate the proposed enhancements in the Context-Aware Simopt-Power (C.A.) framework, we compared it against the baseline Simopt-Power (S.P.) implementation (from [1]) using the Koios benchmark [9]. This benchmark comprises deep-learning circuits of varying complexity, with inputs that are compatible with Verilator, which we use to generate the toggle data from (Simopt-counters). We measured dynamic power reduction, LUT overhead, and area-delay-product to assess the trade-offs arising from context-

TABLE I
POWER-AREA-DELAY COMPARISON FOR SIMOPT-POWER (S.P.) AND CONTEXT-AWARE SIMOPT-POWER (C.A.). AD = AREA·DELAY, PD = POWER·DELAY.

Benchmark	Power			ΔP		Area			ΔA		Delay			ΔD			AD			ΔAD (%)		PD			ΔPD (%)	
	w/o	w/S.P.	w/C.A.	S.P.	C.A.	w/o	w/S.P.	w/C.A.	S.P.	C.A.	w/o	w/S.P.	w/C.A.	S.P.	C.A.	w/o	w/S.P.	w/C.A.	S.P.	C.A.	w/o	w/S.P.	w/C.A.	S.P.	C.A.	
dla_like	1.86	1.69	1.73	8.8	6.7	479619	571931	533264	19.2	11.2	35.10	34.71	1.1	16834627	19851725	18509593	17.9	9.9	65.3	58.7	60.0	10.1	8.0			
clstm_like	0.93	0.86	0.87	8.3	6.5	201945	235509	222978	16.6	10.4	31.14	30.76	1.2	6288567	7244257	6858803	15.2	9.1	29.0	26.5	26.8	8.7	7.6			
deepfreeze	0.45	0.41	0.42	8.9	6.9	75729	83302	81999	10.0	8.3	70	71	1.4	5301030	5914442	5821929	11.6	9.8	31.5	29.1	29.8	7.6	5.3			
tdarknet_like	0.95	0.87	0.89	8.4	6.5	159873	199841	181392	25.0	13.5	78	79	1.3	12470094	15787439	14329968	26.6	14.9	74.1	68.7	70.3	7.2	5.1			
bwave_like	0.08	0.068	0.071	9.7	7.2	521691	632114	591728	25.0	13.4	14.11	13.96	1.1	7361060	9103511	8260523	23.7	12.2	1.1	0.9	1.0	15.9	12.2			
lstm	2.02	1.84	1.88	8.9	6.8	274477	307414	299029	12.0	8.9	27.04	26.72	1.2	7421858	8214102	7990055	10.7	7.7	54.6	49.2	50.2	10.0	8.0			
bnn	0.839	0.774	0.787	7.7	6.2	43754	51630	48510	18.0	10.9	31.09	30.59	1.6	1360312	1579362	1483921	16.1	9.1	26.1	23.7	24.1	9.2	7.7			
lenet	0.012	0.011	0.011	8.6	6.4	23560	30392	27045	29.0	14.8	20.90	20.52	1.8	492404	623644	554963	26.7	12.7	0.3	0.2	0.2	10.0	10.0			
dnnweaver	1.50	1.35	1.39	10.0	7.3	252431	323429	288705	28.1	14.4	84	85	1.2	21204204	27491465	24539925	29.7	15.7	126.0	114.8	118.1	8.9	6.2			
tpu_like	0.094	0.086	0.088	8.5	6.6	597420	704956	662778	18.0	10.9	73.87	73.06	1.1	44131415	51504085	48422561	16.7	9.7	6.9	6.3	6.4	9.5	7.4			
gemm_layer	0.062	0.056	0.058	8.9	6.8	104338	125639	118236	20.4	13.3	73	74	1.4	7616674	9297286	8749464	22.1	14.9	4.5	4.1	4.3	8.4	5.2			
attention_layer	2.20	1.98	2.04	10.0	7.3	353403	392277	383531	11.0	8.5	16.30	16.12	1.1	5760469	6323505	6182520	9.8	7.3	35.9	31.9	32.9	11.0	8.3			
conv_layer	0.042	0.039	0.040	7.3	6.0	137995	155934	150532	13.0	9.1	10.21	10.08	1.3	1408929	1571815	1517363	11.6	7.7	0.4	0.4	0.4	8.3	6.0			
robot_rl	1.88	1.72	1.76	8.8	6.5	28608	31469	30897	10.0	8.0	24.80	24.38	1.7	709478	767214	753269	8.1	6.2	46.6	41.9	42.9	10.1	8.0			
reduction_layer	0.13	0.11	0.12	10.9	8.2	18511	20952	20180	13.2	9.0	16.20	15.89	1.9	299878	332927	320660	11.0	6.9	2.1	1.7	1.9	17.0	9.5			
spm	0.136	0.123	0.126	10.0	7.5	13463	16425	15120	22.0	12.3	18.17	18.17	0.0	244623	298442	274730	22.0	12.3	2.5	2.2	2.3	9.6	7.4			
eltwise_layer	0.042	0.038	0.039	9.5	7.4	15987	19344	17915	21.0	12.1	9.85	9.66	1.9	157472	186863	173059	18.7	9.9	0.4	0.4	0.4	11.3	8.9			
softmax	0.49	0.43	0.45	10.8	7.7	10938	13126	12223	20.0	11.7	39.05	39.05	0.0	427129	512570	477308	20.0	11.7	19.1	16.8	17.6	12.2	8.2			
conv_layer_hls	0.98	0.90	0.91	8.3	6.5	121167	153882	138112	27.0	14.0	20.66	20.39	1.3	2503310	3137654	2816104	25.3	12.5	20.2	18.4	18.6	9.4	8.4			
proxy	0.055	0.050	0.051	9.1	7.3	9255	10551	10131	14.0	9.5	45	45	0.0	416475	474795	455895	14.0	9.5	2.5	2.2	2.3	9.1	7.3			

aware Simopt-Power using reports from the post-place-and-route flow. For place and route, the optimised netlist post C.A. and standard S.P. are exported as (*.blif) into Vivado, with *xc7a200tsbv4841* as the target device to generate the implemented design. Area is captured as LUT utilisation from the implementation reports, whereas delay represents the critical path delay from the post-place-and-route timing reports. Power is estimated using Vivado’s vectored power analysis with switching activity (*.saif) as input obtained from Verilator. The area, power and delay gains/overheads are compared against the baseline implementation of the circuit through standard Vivado implementation flow. As shown in table I, our context-aware flow achieves an average dynamic power reduction of $\approx 6.8\%$ across the benchmark, which is a slight reduction over the original S.P.’s $\approx 9.4\%$ power gain, compared to the baseline implementation. However, we observe a significant improvement in LUT overhead, with C.A. flow incurring only $\approx 11.21\%$ average increase in LUT area compared to the original S.P.’s $\approx 18.63\%$ increase, both measured over the baseline implementation of the circuit (w/o column in table). This improvement is better reflected in the percentage changes in the Power-Delay (PD) product and the Area-Delay (AD) product with respect to the baseline implementation (captured by ΔPD and ΔAD columns respectively). We can see that C.A. achieves nearly the same energy efficiency (PD) as the S.P. implementation at significantly better area efficiency (AD) across all designs, demonstrating its ability for performance favourable trade-off between power reduction and resource utilisation. This can be attributed to the targeted and context-aware nature of the optimisations in C.A., which allows for more efficient use of LUT resources while still achieving meaningful power savings. Overall, the results indicate that our context-aware enhancements provide a more balanced optimisation strategy, delivering respectable power reductions with significantly lower area overhead, thus improving the overall efficiency of the FPGA designs.

IV. CONCLUSION

In this work, we presented **Context-aware Simopt-Power**, an enhanced framework for simulation-driven switching-

activity optimisation in FPGA design flows. By integrating structural design information with simulation-derived activity metadata, we developed a more principled and targeted approach to reducing dynamic power consumption. Our context-aware Shannon splitting heuristic, elimination of heuristic constants, and comprehensive area-delay-product evaluation demonstrated improved trade-offs between power reduction and resource utilisation compared to the original Simopt-Power implementation. Future work will explore further refinements to the decision policy, such as incorporating additional structural features and extending the design choices to be more data and workload-aware.

REFERENCES

- [1] E. Wadhwa and S. Shreejith, “Simopt-power: Leveraging simulation metadata for low-power design synthesis,” in *2025 IEEE Nordic Circuits and Systems Conference (NorCAS)*, 2025, pp. 1–6.
- [2] M. Kubica, B. Pochopień, and D. Kania, “Switching activity reduction of sop networks,” *IEEE Access*, vol. 12, pp. 112 984–112 994, 2024.
- [3] A. L. Hameed, M. M. Akawee, and M. Hameed, “Power reduction using pipeline-clock gating technique in synchronous design with fpga implementation,” in *2022 3rd Information Technology To Enhance e-learning and Other Application (IT-ELA)*, IEEE, 2022, pp. 210–214.
- [4] Y. Xue and J. Huang, “Regate: Enabling power gating in neural processing units,” in *Proceedings of the 58th IEEE/ACM International Symposium on Microarchitecture*, 2025, pp. 1160–1177.
- [5] M. Vaithianathan, M. Patil, S. F. Ng, and S. Udkar, “Low-Power FPGA design techniques for Next-Generation mobile devices,” *ESP International Journal of Advancements in Computational Technology (ESP-IJACT)*, vol. 2, no. 2, pp. 82–93, 2024.
- [6] Y. Bai et al., “Learning to compare hardware designs for high-level synthesis,” ser. MLCAD ’24, Salt Lake City, UT, USA: Association for Computing Machinery, 2024. [Online]. Available: <https://doi.org/10.1145/3670474.3685940>
- [7] D. Padovano, A. Carpegna, A. Savino, and S. Di Carlo, “SpikeExplorer: Hardware-Oriented Design Space Exploration for Spiking Neural Networks on FPGA,” in *Proceedings of Electronics*, vol. 13, 2024, p. 1744. [Online]. Available: <https://www.mdpi.com/2079-9292/13/9/1744>
- [8] E. Wadhwa and S. Shreejith, “Simopt - Simulation Pass for Speculative Optimisation of FPGA-CAD Flow,” in *2024 IEEE International Conference on Omni-layer Intelligent Systems (COINS)*, 2024, pp. 1–6.
- [9] A. Arora et al., “Koios 2.0: Open-source deep learning benchmarks for FPGA architecture and CAD research,” *IEEE Transactions on Computer-Aided Design of Integrated Circuits and Systems*, vol. 42, no. 11, pp. 3895–3909, 2023.